Sensors and Actuators B 258 (2018) 18–24

Contents lists available at ScienceDirect

Sensors and Actuators B: Chemical

journal homepage: www.elsevier.com/locate/snb

Research paper

Combination of periodic hybrid nanopillar arrays and gold nanorods for improving detection performance of surface-enhanced Raman spectroscopy

Nak-hyeon Kim [a,1], Soogeun Kim [b,1], Munsik Choi [b], Hyeong-Ho Park [c], Nam Hoon Kim [d], Sang Yoon Park [a], Kyung Min Byun [b,*], Soo Yeol Lee [b,*]

[a] Advanced Institutes of Convergence Technology, Seoul National University, Suwon 16229, Republic of Korea
[b] Kyung Hee University, College of Electronics and Information, Dept. of Biomedical Engineering, 1732 Deogyeong-daero, Giheung-gu, Yongin 17104, Republic of Korea
[c] Electronic Devices Lab., Device Engineering Labs, Korea Advanced Nano Fab Center, 109 Gwanggyo-ro, Yeongtong-gu, Suwon 16229, Republic of Korea
[d] Center for Convergent Research of Emerging Virus Infection, Korea Research Institute of Chemical Technology, 141 Gajeong-ro, Yuseong-gu, Daejeon 34114, Republic of Korea

ARTICLE INFO

Article history:
Received 15 August 2017
Received in revised form
12 November 2017
Accepted 14 November 2017
Available online 15 November 2017

Keywords:
SERS
Hybrid nanopillar array
Hetero-aggregation
Signal amplification
Line broadening

ABSTRACT

Surface-enhanced Raman spectroscopy (SERS) based on metallic nanoparticles has suffered from poor reproducibility and line broadening of SERS signals. To overcome these problems, we newly propose the SERS substrate incorporating periodic hybrid nanopillar arrays combined with gold nanorods on a flat gold surface. Low reproducibility caused by inhomogeneously distributed and aggregated gold nanoparticles could be improved by employing periodic nanopillar arrays. In addition, we experimentally found that the hybrid nanopillar, in which a dielectric layer is sandwiched between a flat gold film and a gold nanopillar, can reduce line broadening of SERS signals significantly. In this study, the proposed SERS substrate has the potential to provide SERS signals with higher reproducibility and smaller line broadening for high-sensitivity detection of target molecules.

1. Introduction

Since the experimental observation of Raman scattering effect in 1928 [1], Raman spectroscopy has been widely used as a molecular analytical tool in the fields such as chemistry [2,3], biology [4,5], medicine [6,7], forensic science [8] and arts [9,10]. Raman spectroscopy is specialized in non-invasive and non-destructive detection and selective quantification of target materials because Raman scattering signals can provide distinctive spectral patterns according to target materials for molecular identification [11]. It is also worth noticing that Raman spectroscopy is well suited to analysis of aqueous samples since water is a very weak Raman scatterer and typically the peak intensity from a solute is much stronger than those from water, even whpplications have been limited due to very weak signal intensity. In addition, as weak Raman signals are often overwhelmed by fluorescence background signal, many researchers have investigated surface-enhanced Raman spectroscopy (SERS) for the amplification of Raman signal intensity by utilizing localized surface plasmon resonance (LSPR) phenomena. It has been reported that extremely high enhancement could be achieved by employing various metallic nanostructures. Grand et al. found that the amplification of Raman signal intensity strongly depends on the size and shape of metallic nanoparticles because these factors influence the ratio of absorption and scattering events [13]. However, it is still challenging to ensure the spatial reproducibility of SERS signals by fabricating metallic nanoparticles in a controlled manner onto SERS substrates. Spatially non-uniform amplification caused by inhomogeneous distribution of metallic nanoparticles onto SERS substrates can lead to large fluctuations in SERS signals from the SERS substrates, resulting in poor reproducibility of the SERS signals. Also, the detection performance of SERS substrates is often degraded by line broadening of SERS signals, which is attributed to surface complexation of target molecules [14] and/or strong plasmonic field distribution.

* Corresponding authors.
E-mail addresses: kmbyun@khu.ac.kr (K.M. Byun), sylee01@khu.ac.kr (S.Y. Lee).
[1] Authors equally contribute to the research work as 1st author.

https://doi.org/10.1016/j.snb.2017.11.065
0925-4005/

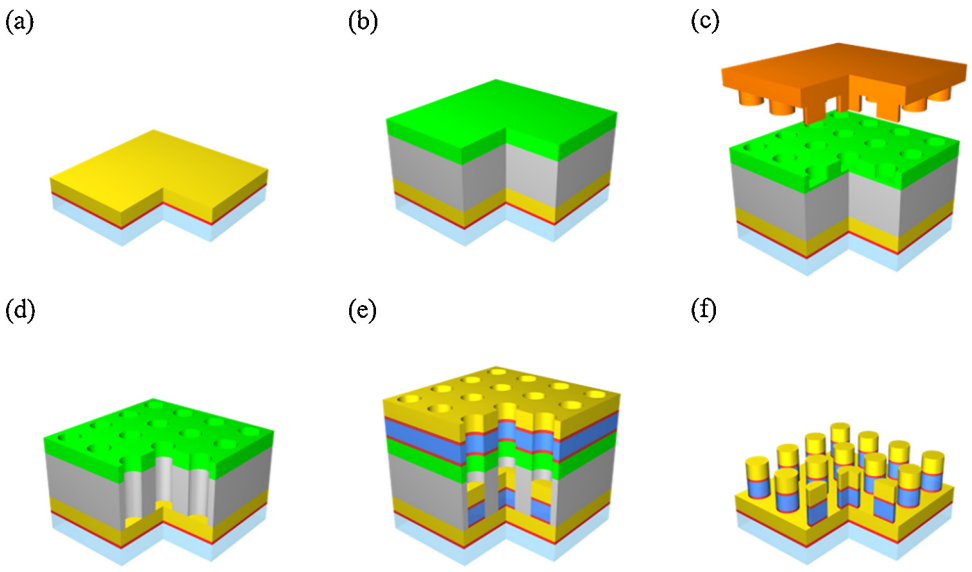

Fig. 1. Fabrication processes for periodic hybrid nanopillar arrays using UV-NIL; (a) deposition of titanium and gold film layers on NSF10 glass, (b) spin-coating of PMMA and imprint resin layers, (c) imprinting of a hole-array pattern by the PUA mold, (d) etching of the PMMA layer, (e) fabrication of the MgF_2/gold hybrid nanopillar arrays, and (f) lift-off of the residual PMMA and imprint resin layers.

In this study, we propose the SERS substrate incorporating periodic dielectric/gold hybrid nanopillar arrays combined with gold nanorods on a flat gold film. Thin gold layer is employed to facilitate a surface-limited binding event. The dielectric layer of magnesium fluoride (MgF_2) in the hybrid nanopillar arrays is introduced to prevent direct interactions between the hybrid nanopillar and the gold nanorods, thereby improving line broadening of SERS signals. The proposed SERS substrate can provide the hetero-aggregation of periodic hybrid nanopillar arrays and gold nanorods, which is intended to obtain the SERS signals with improved reproducibility and peak detection. To investigate the influence of the hetero-aggregation on the quality of SERS signals, we perform the experiments for the three types of SERS substrate; i) only gold nanorods, ii) combination of periodic gold nanopillar arrays and gold nanorods, and iii) combination of periodic MgF_2/gold hybrid nanopillar arrays and gold nanorods. Also, the amplification ratios of each SERS substrate are numerically investigated and compared with experimental results.

2. Materials and methods

2.1. Fabrication of SERS substrate

Fig. 1 shows the fabrication processes for periodic hybrid nanopillar arrays. First of all, an NSF10 glass was prepared through the following procedures. The glass was cleaned using isopropyl alcohol for 10 min, rinsed with deionized water for 10 min, and dried with nitrogen gas. 5-nm thick titanium and 45-nm thick gold layers were sequentially deposited on the glass using an electron-beam evaporator (UEE, Ultech). The titanium layer was used to improve adhesion between the glass and the gold layer. A 350-nm thick polymethyl methacrylate (PMMA) layer was spin-coated on the gold layer at 1000 rpm for 2 min and cured on a hot plate at 170°C for 5 min. Then, a 200-nm thick UV-curable resin layer (NIP-SC28LV400, ChemOptics) was spin-coated on the PMMA layer at 2000 rpm for 1 min. The polyurethane acrylate (PUA) mold, replicated from a silicon master with a 320-nm diameter hole-array pattern (period = 530 nm), was used for imprinting a periodic hole-array pattern on the resin layer. Before imprinting the resin layer using nanoimprint lithography (NIL), trichlorosilane (97%, Sigma-Aldrich) which prevents adhesion between the resin layer and the PUA mold was coated on the PUA mold in advance [15]. The PUA mold was then pressed onto the resin layer by a nanoimprinter (NIL-8 imprinter, Obducat) at 2 MPa for 3 min. The imprint resin layer was exposed to UV light for 2 min for curing of the imprint resin layer by a photochemical reaction. After the imprinting by NIL, residues on the resin layer were removed by a plasma asher (ALA-0601E, AMS) for pattern transfer onto the PMMA layer. Using O_2 reactive ion etching (RIE) (Versaline, Plasma-Therm), the PMMA layer was etched. MgF_2 and gold were then deposited on the surface as dielectric and metallic layers of hybrid nanopillar arrays. For the MgF_2/gold hybrid nanopillar arrays, 10-nm thick titanium, 50-nm thick MgF_2, 10-nm thick titanium, and 50-nm thick gold were deposited in series. On the other hand, for gold nanopillar arrays, 10-nm thick titanium and 50-nm thick gold were deposited. As the final step of the processes, the residual PMMA and imprint resin layers were dissolved in an acetone solution by a lift-off process. The coefficient of variation (CV) for the nanopillar size was measured to be less than 5%, implying that the nanopillar arrays were realized with a great uniformity. The total effective pattern area was approximately $15 \times 15\ mm^2$.

2.2. Attachment of gold nanorods

To realize the hetero-aggregation of periodic nanopillar arrays and gold nanorods, the fabricated substrates were first immersed in 1 mM 2-aminoethanethiol solution for 12 h for chemical reaction between the gold surface and biotins. Then, 340 μM NHS-PEG4-biotin (PN 21329, Thermo Scientific) in a phosphate buffered saline (PBS) solution (pH 7.4) was dropped onto the surface of the fabricated substrates and kept for 2 h. For the hetero-aggregation, streptavidin-conjugated gold nanorods were dropped onto the surface of the fabricated SERS substrates. Due to the strong affinity between biotin and streptavidin, the nanorods were bound to the surface of the fabricated substrates. The morphological structure of SERS substrates was characterized using a field emission scanning electron microscope (FE-SEM) (Leo Supra 55, Carl Zeiss) at 10 kV.

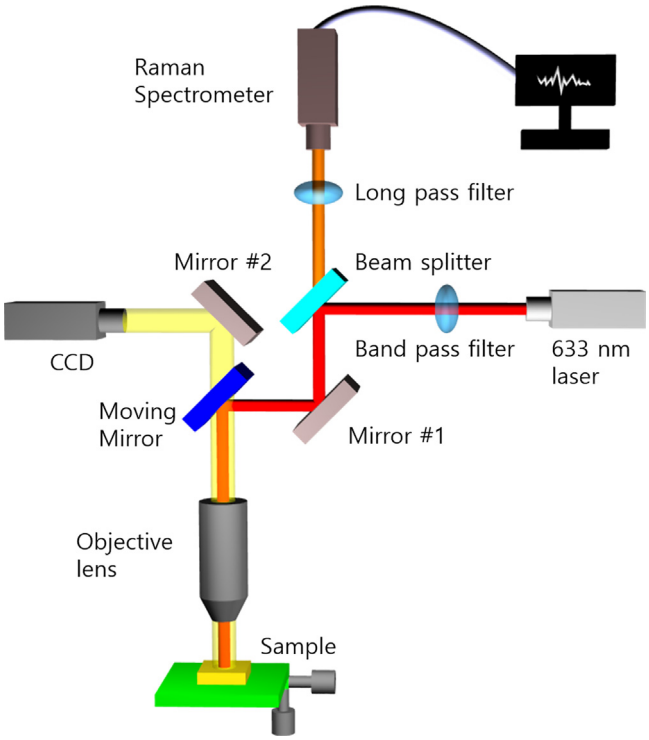

Fig. 2. Schematic of the confocal Raman microscope system.

2.3. SERS measurement

To investigate the characteristics of the three types of SERS substrate, 0.1 mM rhodamine 6G (R6G) was used as a target material. The R6G solution was dropped onto the each SERS substrate surface and kept for 1 h, and then the each surface was cleaned with ethanol and deionized water for 10 min to remove the unfixed target material. SERS signals of R6G were obtained using a confocal Raman microscope system with an excitation source of 633 nm (32413, Research Electro-Optics, Inc., maximum output power = 35 mW) as shown in Fig. 2. The laser spot size on the SERS substrate surface was about 1 μm (Note that the diameter and array period of the nanopillar were 320 nm and 530 nm, respectively). The signals backscattered from the SERS substrate were collected and detected by a 50 × objective lens (NA = 0.75) and a monochromator/spectrograph (MS5004i, Solar TII) with a cooled deep-depletion CCD camera (DU920P-BR-DD, Andor Technology). Each SERS substrate was measured 5 times at different positions in the spectral range of 700–1700 cm^{-1} with the resolution of 0.7 cm^{-1} and the acquisition time of 10 s. The instrument noise signals were simply subtracted from the raw SERS signals and then, the Savitzky-Golay smoothing [16] and improved polynomial baseline correction [17] were carried out sequentially.

3. Results and discussion

Fig. 3 shows FE-SEM images of the three types of SERS substrate. Randomly distributed gold nanorods were formed in the substrate #1 on a flat gold film. Because structural reproducibility and stability of SERS substrate are strongly associated with successful SERS detection, the acquisition quality of SERS signal by the substrate #1 is predicted to be relatively low due to spatial non-uniformity and uncontrollable aggregation [18–20]. On the contrary, the substrate #2 and #3 show the hetero-aggregation of periodic nanopillar arrays and gold nanorods, forming a quasi-periodic distribution. This phenomenon is found in a mixture of two or more types of nanostructure. The hetero-aggregation can be attributed to the different size between the nanopillar and the gold nanorod which induces temporary dipoles by van der Waals forces [21], thereby resulting in attraction between the nanopillar and the gold nanorod. The hetero-aggregated nanostructures are expected to provide not only amplification of Raman signal intensity but also spatially high reproducibility in SERS detection.

Fig. 4 shows the SERS signals of R6G obtained from the three types of SERS substrate. All SERS signals included Raman peaks of R6G molecule; C—H out-of-plane bend mode at around 771 cm^{-1}, C—H in-plane bend mode at around 1186 cm^{-1}, C—C and C—N stretching mode at around 1311 cm^{-1} and 1362 cm^{-1}, aromatic C—C stretching mode at around 1510 cm^{-1}, 1586 cm^{-1}, and 1651 cm^{-1} [22–24]. The average SERS signal amplification ratios of the substrate #2 and #3 to that of the substrate #1 were obtained to be 4.56 ± 0.99 and 3.46 ± 0.88, respectively, using individual amplification ratio values of seven primary Raman peaks of R6G. These results indicate that the combination of periodic nanopillar arrays and gold nanorods effectively amplifies the Raman signal inten-

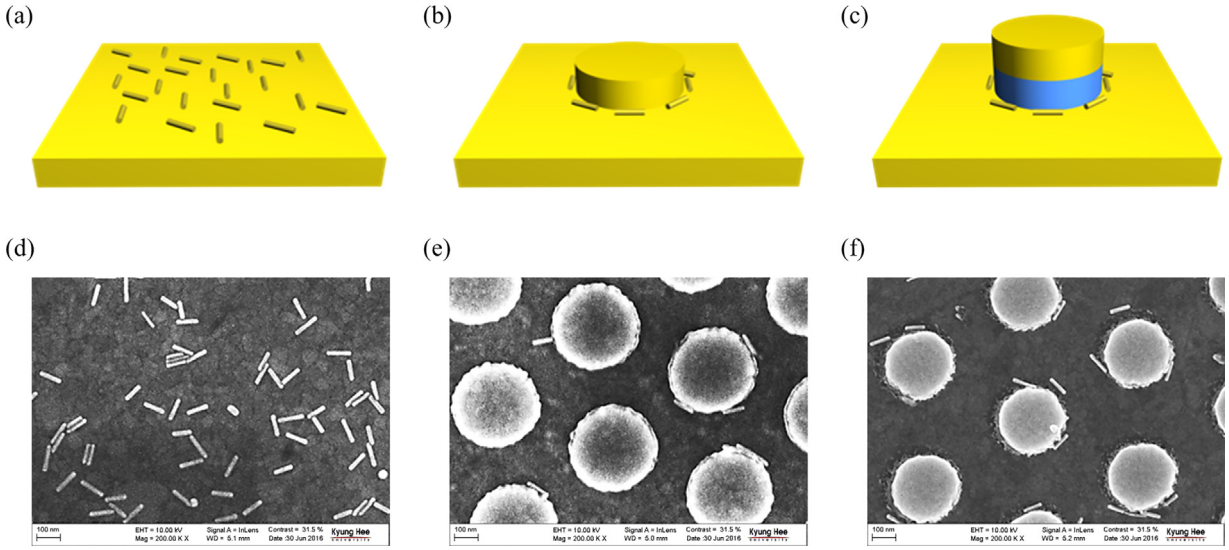

Fig. 3. Schemes and FE-SEM images of the three types of SERS substrate; (a,d) only gold nanorods (substrate #1), (b,e) combination of periodic gold nanopillar arrays and gold nanorods (substrate #2), (c,f) combination of periodic MgF_2/gold hybrid nanopillar arrays and gold nanorods (substrate #3).

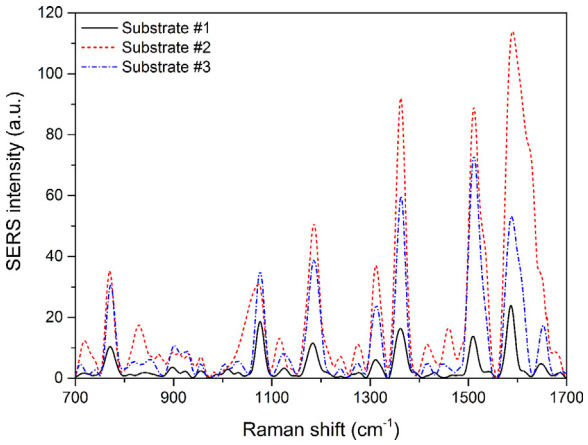

Fig. 4. SERS signals of R6G at each SERS substrate.

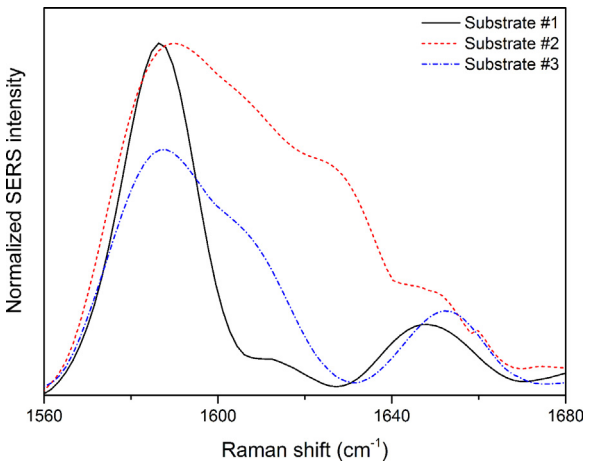

Fig. 6. Line broadening of the Raman peaks at around 1586 cm^{-1} and 1651 cm^{-1}.

sity. The amplification level of SERS signal is typically determined by the density, size, and shape of metal nanostructures, but can also be determined by the interactions among target materials, metallic surfaces, and microenvironment [25]. For the substrates #2 and #3, the interactions among R6G, the flat gold film, gold nanorods, and nanopillars appear to be dominant for the amplification of Raman signal intensity. However, especially for the substrate #3, the interactions between the gold nanorods and the nanopillars are prevented by the dielectric layer of MgF_2 so that the amplification is slightly decreased when compared with the substrate #2.

Near-field simulations using finite-difference time-domain (FDTD) method were performed in order to investigate the electromagnetic field distribution near the surface of the three types of SERS substrate. The computation results in Fig. 5 show that strong electromagnetic field occurs at the corners of the nanopillar. For the gold nanopillar of Fig. 5b, great enhancement of electromagnetic field is found between gold nanopillar and gold nanorods, while it is not observed for the hybrid nanopillar due to the presence of dielectric layer, as shown in Fig. 5c. When the summation of electromagnetic field amplitude over the surface was calculated, the maximum of 1166 was obtained at the SERS substrate #2. On the other hand, the summation values were determined as 313 and 1076 for the SERS substrate #1 and #3, respectively. When it is assumed that R6G was homogeneously distributed on the substrate surface, we can predict that the SERS signal is the strongest at the substrate #2 because the amplification of Raman signal is correlated to field-matter interaction, which is consistent with the trend of experimental results in Fig. 4.

The min-max normalized SERS signals were used to evaluate the signal quality in SERS detection [26]. Line broadening of SERS signals can be attributed to surface complexation of target molecules [14] and/or strong plasmonic field distribution. In this study, because it is likely that R6G was almost uniformly distributed on the SERS substrates, it is expected that the strong plasmonic field distribution rather than surface complexation of R6G would be dominant for the line broadening of SERS signals. As shown in Fig. 6, substantial line broadening of Raman peaks is observed at around 1586 cm^{-1} and 1651 cm^{-1} and even the two Raman peaks are overlapped for the substrate #2. This overlap can be removed by adding the dielectric layer of MgF_2 between the flat gold film and the gold nanopillar. In the case of the substrate #2, the plasmonic field enhancement can occur by the interactions among flat gold film, gold nanorod, and gold nanopillar. On the other hand, for the substrate #3, only interaction between gold film and gold nanorod occurs because the added dielectric layer disrupts an interaction between the gold nanorod and the gold nanopillar. While plasmonic field enhancement is decreased compared with the case of the substrate #2, it may lead to an improvement of the line broadening for the substrate #3. As a result, we can reduce the line broadening due to the strong plasmonic field distribution by presenting the dielectric layer between gold film and gold nanopillar.

To analyze the spatial reproducibility of SERS signals according to the type of SERS substrate, relative standard deviation (RSD) and margin of error (MOE) for the seven primary Raman peaks of R6G were calculated and compared using the normalized SERS signals. Fig. 7a shows the normalized and averaged SERS signals of R6G for the three types of SERS substrate. Each SERS signal represents the average (solid lines) and standard deviation (filled areas) calculated from 5 SERS signals measured at different positions for each SERS substrate. In Fig. 7a, it is instinctively found that the standard deviations of SERS signals of the substrate #2 and #3 are smaller than that

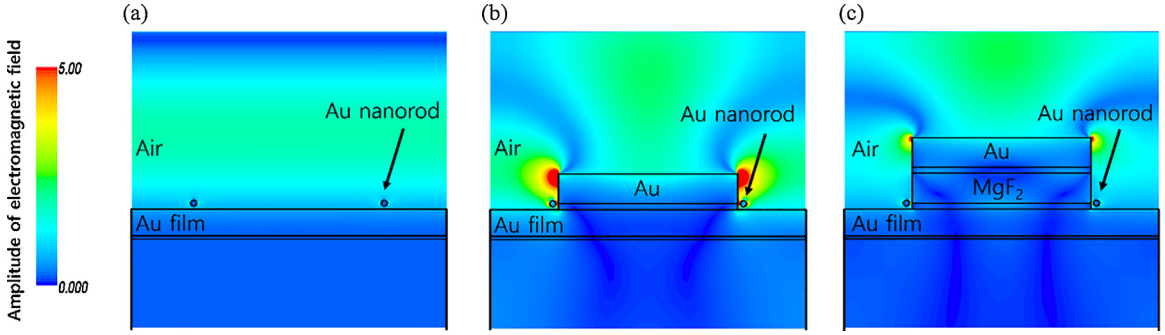

Fig. 5. Simulation results about the electromagnetic field distribution at each SERS substrate; the summation of electromagnetic field amplitude over the surface of each SERS substrate is (a) 313 for the substrate #1, (b) 1166 for the substrate #2, and (c) 1076 for the substrate #3.

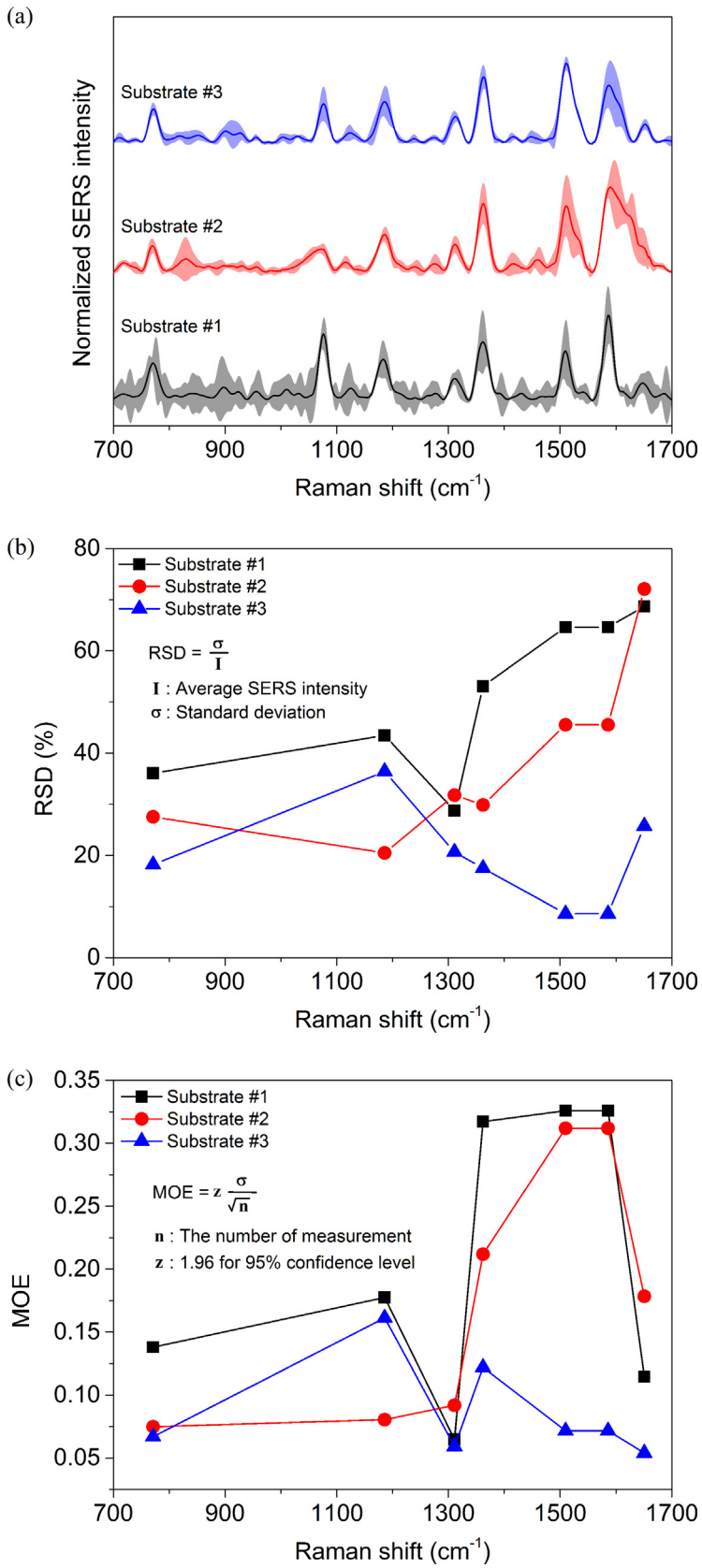

Fig. 7. (a) Normalized and averaged SERS signals of R6G (line: average, filled area: standard deviation) and (b) relative standard deviation (RSD) and (c) margin of error for the seven primary Raman peaks of R6G (771 cm^{-1}, 1186 cm^{-1}, 1311 cm^{-1}, 1362 cm^{-1}, 1510 cm^{-1}, 1586 cm^{-1}, and 1651 cm^{-1}) for each SERS substrate.

of the substrate #1, which implies that the spatial reproducibility of SERS signals is improved. Better reproducibility in the substrates #2 and #3 is attributed to the quasi-periodic distribution by the periodic nanopillar arrays and gold nanorods because spatial uniformity and controllable distribution of nanostructures are strongly associated with the stable and steady amplification of Raman signal intensity. In order to quantitatively present the results of the improved reproducibility, the RSD and MOE values of each SERS substrate were plotted in Fig. 7b and c, respectively, for the seven primary Raman peaks of R6G (771 cm^{-1}, 1186 cm^{-1}, 1311 cm^{-1}, 1362 cm^{-1}, 1510 cm^{-1}, 1586 cm^{-1}, and 1651 cm^{-1}). When compared with the RSD of substrate #1, while the RSD of substrate #3 was decreased at all Raman peaks of R6G, it was not consistent for the RSD of substrate #2. Note that an increased RSD was found at the peaks of 1311 cm^{-1} and 1651 cm^{-1} of substrate #2. The MOE data in Fig. 7c were highly consistent with the results of RSD. Especially, the incremental trend of RSD and MOE of substrate #2 at 1651 cm^{-1} is attributed to the disappearance of the Raman peak by the overlap of the peaks at 1586 cm^{-1} and 1651 cm^{-1}. These results imply that line broadening is highly associated with the reproducibility in SERS detection. The SERS substrate #3 that can provide the quasi-periodic distribution and hetero-aggregation of periodic MgF_2/gold hybrid nanopillar arrays and gold nanorods showed the potential of SERS detection of high reproducibility and improved line broadening.

4. Conclusion

In this study, the SERS substrate consisting of periodic MgF_2/gold hybrid nanopillar arrays and gold nanorods have been newly developed. The hetero-aggregation of periodic hybrid nanopillar arrays and gold nanorods was effective not only for amplifying Raman signal intensity but also for improving the reproducibility and line broadening in SERS detection. Based on the theoretical and experimental results, the proposed SERS substrate is expected to be applicable to the fields of analysis of specific small molecules where the high quality in SERS detection is required.

Disclosures

All authors declare no conflicts of interest or financial relationships to disclose.

Acknowledgments

This work was supported by the National Research Foundation of Korea (NRF) grant funded by the Korean Government (2016K1A3A1A32913187 and 2017R1A2B4012428) and by Basic Science Research Program through the NRF funded by the Ministry of Education (NRF-2017R1D1A1B03035950). Nam Hoon Kim was supported by the National Research Council of Science & Technology (NST) grant by the Korea government (MSIP) (No. CRC-16-01-KRICT). This work was also supported by the Kyung Hee University Research Fund in 2015 (KHU-20150800).

References

[1] C.V. Raman, A new radiation, Indian J. Phys. 2 (1928) 387–398.
[2] O. Lyandres, N.C. Shah, C.R. Yonzon, J.T. Walsh, M.R. Glucksberg, R.P. Van Duyne, Real-time glucose sensing by surface-enhanced Raman spectroscopy in bovine plasma facilitated by a mixed decanethiol/mercaptohexanol partition layer, Anal. Chem. 77 (2005) 6134–6139.
[3] G. Sabatté, R. Keir, M. Lawlor, M. Black, D. Graham, W.E. Smith, Comparison of surface-enhanced resonance Raman scattering and fluorescence for detection of a labeled antibody, Anal. Chem. 80 (2008) 2351–2356.
[4] M. Larsson, J. Lindgren, Analysis of glutathione and immunoglobulin G inside chromatographic beads using surface-enhanced Raman scattering spectroscopy, J. Raman Spectrosc. 36 (2005) 394–399.
[5] A. Rasmussen, V. Deckert, Surface- and tip-enhanced Raman scattering of DNA components, J. Raman Spectrosc. 37 (2006) 311–317.
[6] J. Binoy, I.H. Joe, V.S. Jayakumar, O.F. Nielsen, J. Aubard, DFT based relaxed PES scan studies and SERS of anti cancer drug, Combretastatin A-4, Laser Phys. Lett. 2 (2005) 544–550.
[7] S. Cîntă-Pînzaru, N. Peica, B. Küstner, S. Schlücker, M. Schmitt, T. Frosch, J.H. Faber, G. Bringmann, J. Popp, FT-Raman and NIR-SERS characterization of the antimalarial drugs chloroquine and mefloquine and their interaction with hematin, J. Raman Spectrosc. 37 (2006) 326–334.
[8] J.M. Sylvia, J.A. Janni, J.D. Klein, K.M. Spencer, Surface-enhanced Raman detection of 2,4-dinitrotoluene impurity vapor as a marker to locate landmines, Anal. Chem. 72 (2000) 5834–5840.
[9] K. Chen, K.C. Vo-Dinh, F. Yan, M.B. Wabuyele, T. Vo-Dinh, Direct identification of alizarin and lac dye on painting fragments using surface-enhanced Raman scattering, Anal. Chim. Acta. 569 (2006) 234–237.
[10] K. Chen, M. Leona, K.C. Vo-Dinh, F. Yan, M.B. Wabuyele, T. Vo-Dinh, Application of surface-enhanced Raman scattering (SERS) for the identification of anthraquinone dyes used in works of art, J. Raman Spectrosc. 37 (2006) 520–527.
[11] E. Smith, G. Dent, Modern Raman Spectroscopy – A Practical Approach, John Wiley & Sons, Ltd, Chichester, 2005.
[12] G.A. Hope, R. Woods, C.G. Munce, Raman microprobe mineral identification, Miner. Eng. 14 (2001) 1565–1577.
[13] J. Grand, M. Lamy de la Chapelle, J.-L. Bijeon, P.-M. Adam, A. Vial, P. Royer, Role of localized surface plasmons in surface-enhanced Raman scattering of shape-controlled metallic particles in regular arrays, Phys. Rev. B 71 (2005) 033407.
[14] Y. Fleger, Y. Mastai, M. Rosenbluha, D.H. Dresslerb, SERS as a probe for adsorbate orientation on silver nanoclusters, J. Raman Spectrosc. 40 (2009) 1572–1577.
[15] J.Y. Kim, D.G. Choi, J.H. Jeong, E.S. Lee, UV-curable nanoimprint resin with enhanced anti-sticking property, Appl. Surf. Sci. 254 (2008) 4793–4796.
[16] J. Addis, N. Mohammed, O. Rotimi, D. Magee, A. Jha, V. Subramanian, Raman spectroscopy of endoscopic colonic biopsies from patients with ulcerative colitis to identify mucosal inflammation and healing, Biomed. Opt. Express 7 (2016) 2022–2035.
[17] J. Zhao, H. Lui, D.I. McLean, H. Zeng, Automated autofluorescence background subtraction algorithm for biomedical Raman spectroscopy, Appl. Spectrosc. 61 (2007) 1225–1232.
[18] C.Y. Fu, K.W. Kho, U.S. Dinish, Z.Y. Koh, O. Malini, Enhancement in SERS intensity with hierarchical nanostructures by bimetallic deposition approach, J. Raman Spectrosc. 43 (2012) 977–985.
[19] C. Zhu, G. Meng, Q. Huang, Z. Huang, Vertically aligned Ag nanoplate-assembled film as a sensitive and reproducible SERS substrate for the detection of PCB-77, J. Hazard. Mater. 211 (2012) 389–395.
[20] S.L. Kleinman, R.R. Frontiera, A.I. Henry, J.A. Dieringer, R.P. Van Duyne, Creating characterizing, and controlling chemistry with SERS hot spots, Phys. Chem. Chem. Phys. 15 (2013) 21–36.
[21] A.M. Islam, B.Z. Chowdhry, M.J. Snowden, Heteroaggregation in colloidal dispersions, Adv. Colloid Interface Sci. 62 (1995) 109–136.
[22] Y. Lu, G.L. Liu, L.P. Lee, High-density silver nanoparticle film with temperature-controllable interparticle spacing for a tunable surface enhanced Raman scattering substrate, Nano Lett. 5 (2005) 5–9.
[23] M. Baia, L. Baia, S. Astilean, Gold nanostructured films deposited on polystyrene colloidal crystal templates for surface-enhanced Raman spectroscopy, Chem. Phys. Lett. 404 (2005) 3–8.
[24] T.T.B. Quyen, C.C. Chang, W.N. Su, Y.H. Uen, C.J. Pan, J.Y. Liu, J. Rick, K.Y. Lin, B.J. Hwang, Self-focusing Au@ SiO2 nanorods with rhodamine 6G as highly sensitive SERS substrate for carcinoembryonic antigen detection, J. Mat. Chem. B 2 (2014) 629–636.
[25] S.C. Luo, K. Sivashanmugan, J.D. Liao, C.K. Yao, H.C. Peng, Nanofabricated SERS-active substrates for single-molecule to virus detection in vitro: a review, Biosens. Bioelectron. 61 (2014) 232–240.
[26] R. Gautam, S. Vanga, F. Ariese, S. Umapathy, Review of multidimensional data processing approaches for Raman and infrared spectroscopy, EPJ Tech. Instrum. 2 (2015) 1–38.

Biographies

Nak-hyeon Kim received the Ph.D. degree in the Department of Biomedical Engineering, Kyung Hee University in 2015. From 2015–2016, he worked as a research professor in Korea University Guro Hospital. He is currently a senior researcher at the Advanced Institutes of Convergence Technology, Seoul National University. His main research activities are theoretical and experimental studies on high-sensitivity plasmonic biosensors based on metallic nanostructures.

Soogeun Kim is a research professor at the Kyung Hee University, Republic of Korea. He received his MS and PhD degrees in mechatronics from the Gwangju Institute of Science and Technology in 2007 and 2015, respectively. His research interests focus on laser-tissue interaction phenomena and their applications, and ongoing research includes Raman spectroscopy for cancer detection, fiber-optic-based Raman spectroscopy and spectrum data analysis by neural networks.

Kyung Min Byun received the B.S. and M.S. degrees from the school of electrical engineering, Seoul National University, Seoul, Korea, and the Ph.D. degree from Seoul

National University, in 2007. From July 2007 to February 2008, he worked as a visiting scientist in the department of biomedical engineering, Cornell University, Ithaca, NY. He is currently working as associate professor at the department of biomedical engineering, Kyung Hee University, Yongin, Korea. His main research activities are theoretical and experimental studies on high-sensitivity plasmonic biosensors with metallic nanostructures, Raman spectroscopy, and minimally invasive neuromodulation technique based on optical and ultrasound stimulation.

Soo Yeol Lee received the M.S. and Ph.D. degrees in electronics engineering from the Korea Advanced Institute of Science and Technology, Seoul, South Korea, in 1985 and 1989, respectively. He was with the Department of Biomedical Engineering, Konkuk University, South Korea, from 1992 to 1999. In 1999, he joined the Department of Biomedical Engineering, Kyung Hee University, where he is currently the Director of the Functional and Metabolic Imaging Research Center. His current research interests include MRI, CT, elastography, and medical image/signal processing.